Journal of Pharmaceutical Analysis 11 (2021) 757–763

Contents lists available at ScienceDirect

Journal of Pharmaceutical Analysis

journal homepage: www.elsevier.com/locate/jpa

Original article

Spectroscopic studies of the interaction between phosphorus heterocycles and cytochrome P450

Dumei Ma [a, b, 1], Libo Zhang [b, 1], Yingwu Yin [a, *], Yuxing Gao [c, **], Qian Wang [b]

[a] Department of Chemical and Biochemical Engineering, College of Chemistry and Chemical Engineering, Xiamen University, Xiamen, 361005, Fujian, China
[b] Department of Chemistry and Biochemistry, University of South Carolina, Columbia, SC, 29208, USA
[c] Department of Chemistry and Key Laboratory for Chemical Biology of Fujian Province, College of Chemistry and Chemical Engineering, Xiamen University, Xiamen, 361005, Fujian, China

ARTICLE INFO

Article history:
Received 27 April 2020
Received in revised form
11 December 2020
Accepted 17 December 2020
Available online 21 December 2020

Keywords:
Phosphorus heterocycles
Cytochrome P450
OleT
Interaction
Spectroscopy

ABSTRACT

P450 fatty acid decarboxylase OleT from *Staphylococcus aureus* ($OleT_{SA}$) is a novel cytochrome P450 enzyme that catalyzes the oxidative decarboxylation of fatty acids to yield primarily terminal alkenes and CO_2 or minor α- and β-hydroxylated fatty acids as side-products. In this work, the interactions between a series of cycloalkyl phosphorus heterocycles (CPHs) and $OleT_{SA}$ were investigated in detail by fluorescence titration experiment, ultraviolet–visible (UV–vis) and ^{31}P NMR spectroscopies. Fluorescence titration experiment results clearly showed that a dynamic quenching occurred when CPH-6, a representative CPHs, interacted with $OleT_{SA}$ with a binding constant value of 15.2×10^4 M^{-1} at 293 K. The thermodynamic parameters (ΔH, ΔS and ΔG) showed that the hydrogen bond and van der Waals force played major roles in the interaction between $OleT_{SA}$ and CPHs. The UV–vis and ^{31}P NMR studies indicated the penetration of CPH-6 into the interior environment of $OleT_{SA}$, which greatly affects the enzymatic activity of $OleT_{SA}$. Therefore, our study revealed an effective way to use phosphorus heterocyclic compounds to modulate the activity of cytochrome P450 enzymes.

1. Introduction

Organophosphorus compounds widely exist in biological systems and have drawn largely attentions in medicinal application [1–9]. They have been used for the treatment of human diseases including Alzheimer's, schistosomiasis and osteoporosis [10,11]. Phosphorus heterocycles are heterocyclic compounds containing hetero (O, N) and phosphorus atoms. They have obtained widespread interests because of their potential pharmaceutic applications [12–16]. For example, the oxazaphosphorine ifosfamide (I, Fig. 1) is commonly used as an alkylating chemotherapeutic agent in oncology such as lung, cervical, testicular cancers, and bone or soft tissue sarcomas [12]. A group of new nonpeptidic cyclic phosphon-based hydroxamic acids (II, Fig. 1) have been employed as inhibitors of metalloproteinases [14]. In another example, benzoxaphosphol-2-ones (III, Fig. 1) were designed and prepared, which show significant antibacterial activities [15]. [1,2]oxaphosphinane (IV, Fig. 1) was reported to have an antiproliferative activity against a large panel of NCI cancer cell lines [16]. In addition, interactions of phosphorus heterocyclic compounds with biomacromolecules have been reported, suggesting important biological and pharmaceutical values of these derivatives [17,18].

Cytochromes P450 (P450s) are widely found in a variety of species throughout the biosphere [19]. As a large family of heme-containing redox enzymes, they play an important role in the synthesis of many molecules such as steroid hormones, cholesterol and other fats and acids. Additional P450s serve to metabolize and detoxify exogenous compounds presented to the organism [20–24]. Studying the interaction between drugs and P450s is significant not only for drugs' pharmacological characteristic analysis but also for the enzyme inhibitor/activator discovery [25]. Identification of effective binders to P450s is crucial in distinguishing the risk of drug-drug interactions, where a compound potentially influences the metabolism of other compounds [26]. Moreover, investigations on the interactions of small molecules and P450s will provide insights into the mechanisms of drug action as well as the design of novel medicines.

Peer review under responsibility of Xi'an Jiaotong University.
* Corresponding author.
** Corresponding author.
E-mail addresses: ywyin@xmu.edu.cn (Y. Yin), gaoxingchem@xmu.edu.cn (Y. Gao).
[1] These authors contributed equally to this work.

https://doi.org/10.1016/j.jpha.2020.12.004

Fluorescence spectroscopy is a powerful tool to explore the interactions between small molecules and P450s, which can reveal valuable information of the binding features of small molecules to proteins. Several studies have been investigated, indicating that the fluorescence quenching of P450 enzymes could be triggered by a variety of molecules [27–30]. Mitra and co-workers [27] employed steady-state and time-resolved fluorescence spectroscopy to study the binding of camphor in the active side of cytochrome P450cam. Shumyantseva et al. [28] utilized similar fluorescence assays to detect the existence of riboflavin binding site on cytochrome P450 2B4. In addition, cytochrome P450 CYP1A2 and CYP2D6 were selected to study their interaction with puerarin by Shao et al. by using different spectroscopic studies [29]. Guengerich and co-workers [30] focused on the binding relationship of 7,8-benzoflavone to human cytochrome P450 3A4, revealing the complex fluorescence quenching and binding mechanism.

Recently, we reported a novel method to synthesize a series of cycloalkyl phosphorus heterocycles (CPHs) [31]. Their biological applications are yet to be discovered. Interestingly, these molecules display specific fluorescence and environment responsive properties (e.g. polarity, as shown in Fig. S1), making them excellent probes for small molecule/P450s binding study. OleT is a new P450 enzyme first reported by Rude et al. [32] in 2011. Collective effort has been made to improve the enzyme's catalytic efficiency including the use of small non-polar molecules to stimulate its activity [33–35]. Detailed binding mechanisms are needed to further understand the stimulation effect. Herein, we studied the interactions between CPHs and P450 fatty acid decarboxylase OleT from *Staphylococcus aureus* ($OleT_{SA}$) by using fluorescence spectrum, UV–vis spectrum and ^{31}P nuclear magnetic resonance (NMR) spectroscopies. The effect of CPHs on $OleT_{SA}$ enzymatic activity was also tested. To the best of our knowledge, it is the first work to describe the interaction of phosphorous heterocycles with P450s, which will provide useful information for phosphorus heterocycles' potential biological application. The binding mechanisms illustrated in this work also guide us to design novel stimulator to leverage OleT.

2. Materials and methods

2.1. Materials

The CPHs used here were prepared according to the synthetic method reported previously by our group [31]. The substrate diaryl (arylethynyl)phosphine oxide **1** was reacted with commercially available cycloalkane **2** in the presence of di-*tert*-butyl peroxide (DTBP) (Fig. 2), delivering excellent yield of CPHs. The crude product was purified by chromatographic techniques. The stock solutions of synthesized molecules were prepared by dissolving them in dimethyl sulfoxide (DMSO) to make the concentration as 30 mM. A phosphate buffer (200 mM K_2HPO_4, 100 mM NaCl, pH 7.4) was used unless otherwise noted. Other chemicals used were of analytical reagent grade and double-distilled water was used throughout.

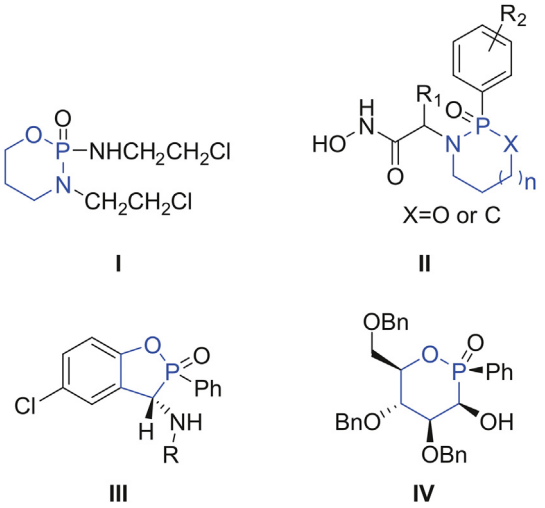

Fig. 1. Structure of representative phosphorus heterocycles as novel pharmaceuticals.

$OleT_{SA}$ expression and purification were performed by following the published paper [36]. Briefly the kanamycin-resistant plasmid T5 containing the $OleT_{SA}$-His6 gene was transformed to BL21 (DE3) containing the chloramphenicol-resistant pTF2 plasmid which has GroEL/GroES/Tig chaperones encoded. A modified terrific broth (TB) (24 g/L yeast extract, 12 g/L tryptone, and 4 g/L peptone) supplemented with 50 μg/mL kanamycin and 20 μg/mL chloramphenicol was used for culturing. 125 mg/L thiamine, and trace metals, 100 μM isopropyl β-D-1-thiogalactopyranoside (IPTG), 10 ng/mL tetracycline and 10 mg/L 5-aminolevulinic acid were added for protein expression. The expression was made at 18 °C for 16–18 h. Nickel-nitriloacetic acid (Ni-NTA) affinity chromatography was used for the purification of the protein, followed by Butyl-S-Sepharose column [37]. Fractions with an Rz value (Abs418 nm/Abs280 nm) above 1.2 were pooled and dialyzed against 200 mM KPi buffer (pH 7.4). Proteins were stored at −80 °C until further use.

2.2. Apparatus

Fluorescence data were collected using Cary-Eclipse Fluorescence Spectrophotometer (Palo Alto, CA, USA) equipped with an attached Cary Temperature Controller. UV–vis spectra were carried on HP 8453 spectrophotometer (Palo Alto, CA, USA). The ^{31}P NMR spectra were obtained with a Bruker Avance 400 spectrometer at 298 K (Bruker, Faellanden, Switzerland).

2.3. Methods

2.3.1. Fluorescence spectroscopy

Fluorescence spectra of $OleT_{SA}$ (~10 μM) were detected with varying the CPHs concentration (0, 5, 10, 15, 20, 25, 30 μM). With 280 nm excitation, the emission spectra were collected in the wavelength range from 300 to 500 nm at 293 K, 298 K, and 303 K, respectively. The different initial fluorescence intensity of the enzyme in all kinds of CPHs system were caused by the different concentration of $OleT_{SA}$. In addition, the fluorescence spectra of CPH-6 were carried out by keeping the concentration of CPH-6 at 30 μM, meanwhile varying the $OleT_{SA}$ concentration (0, 0.2, 0.6, 2, 4, 6, 8 and 10 μM). The spectra were measured in the range of 270–500 nm at the excitation wavelength (λ_{em}) of 250 nm at 298 K. All the experiments were carried out in a conventional quartz cell using phosphate buffered saline (PBS).

2.3.2. UV–vis spectroscopy

Optical spectra were performed using 10 μM $OleT_{SA}$ and the sequential addition of CPH-6 from the 30 mM stock solution. The absorption spectra were collected from 300 nm to 700 nm at 303 K.

2.3.3. ^{31}P NMR study

CPH-6 (50 or 100 μM) in 600 μL D_2O was placed in a 10 mm NMR tube, followed by adding $OleT_{SA}$ (50 μM) and the ^{31}P NMR spectrum was recorded. Bovine serum albumin (BSA) was chosen as a protein control.

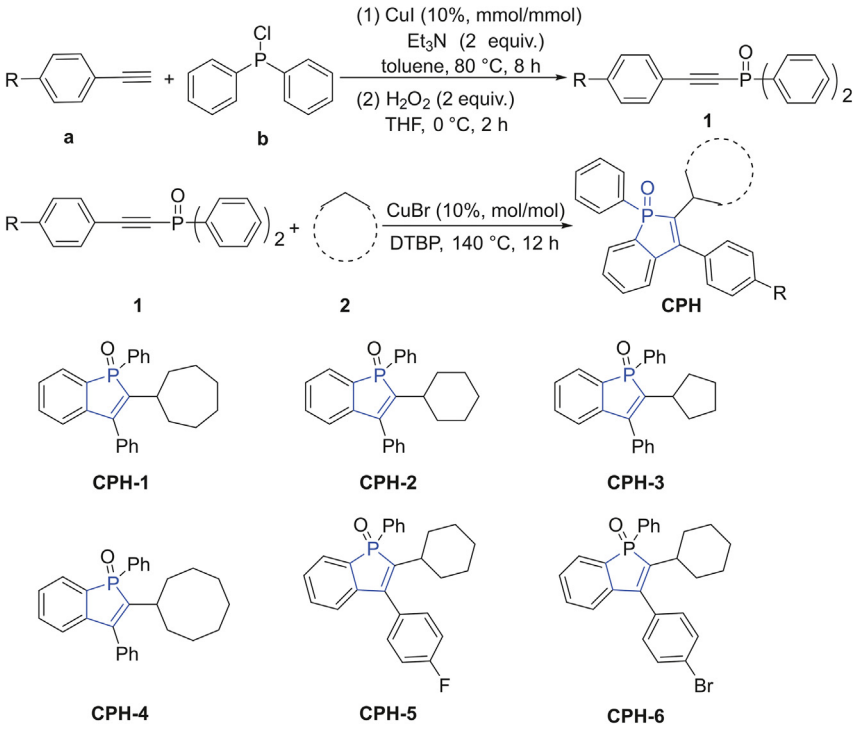

Fig. 2. Synthesis of cycloalkyl phosphorus heterocycles (CPHs).

2.3.4. OleT_{SA} assay

The reaction mixtures (500 μL) containing 5 μM OleT_{SA}, 2 mM hydrocinnamic acid, 2 mM H_2O_2 in the presence and absence of 200 μM phosphorus heterocyclic compounds were incubated at room temperature for 30 min. The reactions were quenched by addition of 1% acetic acid followed by 1,2,3,4-tetramethylbenzene as the internal standard. After centrifuging at 12,000 r/min for 20 min, the supernatant was extracted and tested on HPLC.

3. Results and discussion

3.1. Fluorescence quenching analysis

Intrinsic fluorescence of proteins is caused by three amino acids residues (tryptophan, tyrosine, and phenylalanine) containing aromatic groups. Among them, the tryptophan residues are believed to be main contributors [38]. A very significant aspect of proteins' intrinsic fluorescence is that its tryptophan residues have strong sensitivity to local environment [39–41]. The changes of fluorescence of tryptophan have been a useful tool to reveal the process of protein folding, aggregation and conformation transition [40]. As a result, the proteins' intrinsic fluorescence spectrum responding to small molecules can reflect valuable information about their interactions. In our study, the analysis of OleT_{SA} fluorescence with increasing concentration of all derivatives (0, 5, 10, 15, 20, 25, and 30 μM, respectively) at 298 K was monitored. As shown in Fig. 3, decrease of fluorescence intensity was observed for all derivatives, indicating that the interaction between OleT_{SA} and the CPHs can quench the enzyme's fluorescence signal. In addition, many CPHs in our research showed fluorescence signal at 400–500 nm with 280 nm excitation. In Fig. 3, with higher concentration of CPH-1, a stronger fluorescence signal was observed at 450 nm.

To gain insights into the interaction mechanism of CPHs with OleT_{SA}, CPH-6 was chosen as a model for further investigation. The emission spectra of the compound CPH-6 with various concentrations of OleT_{SA} at 298 K were collected (Fig. 4A). Under 250 nm excitation, CPH-6 emitted fluorescence signal in the range of 380–440 nm, which decreased with the increasing concentration of OleT_{SA}. The result indicated that the fluorescence of the molecule could also be quenched by OleT_{SA}, which could be attributed to the highly hydrophobic environment of the enzyme pocket.

The fluorescence data were further analyzed to reveal the origins of the quenching. It is known that dynamic quenching is the process of inactivation of the excited state of fluorophores after interaction with quenching molecules [42]. However, static quenching often generates nonfluorescent complex of the fluorophore and the quencher. The discrimination of dynamic and static quenching depends on the relationship of quenching constant and temperature [42]. The dynamic quenching constant increases with the rise of temperature while the other one shows the decline of quenching constant with the increase of temperature. The Stern-Volmer equation (Eq. (1)) can be applied to explain the quenching mechanism.

$$\frac{F_0}{F} = 1 + K_q\tau_0[OleT] = 1 + K_{sv}[OleT] \quad (1)$$

Here, F_0 and F represent the fluorescence intensities of OleT without and with a quencher, [*OleT*] refers to the concentration of OleT, K_q means the biomolecular quenching rate constant, K_{SV} is the Stern-Volmer constant, τ_0 is the average lifetime of the molecule without quencher. The average fluorescence lifetime of the biomolecule is evaluated at about 10 ns [43,44], so the quenching constant K_q could be obtained according to the Eq. (2).

$$K_q\tau_0 = K_{sv} \quad (2)$$

The plots of F_0/F versus [*OleT*] are shown in Fig. 4B. The values of K_{SV} and K_q were determined by the slope of the plots and Eq. (2). The results are listed in Table 1 together with the correlation coefficients. As shown in Table 1, a significant increase in Stern-

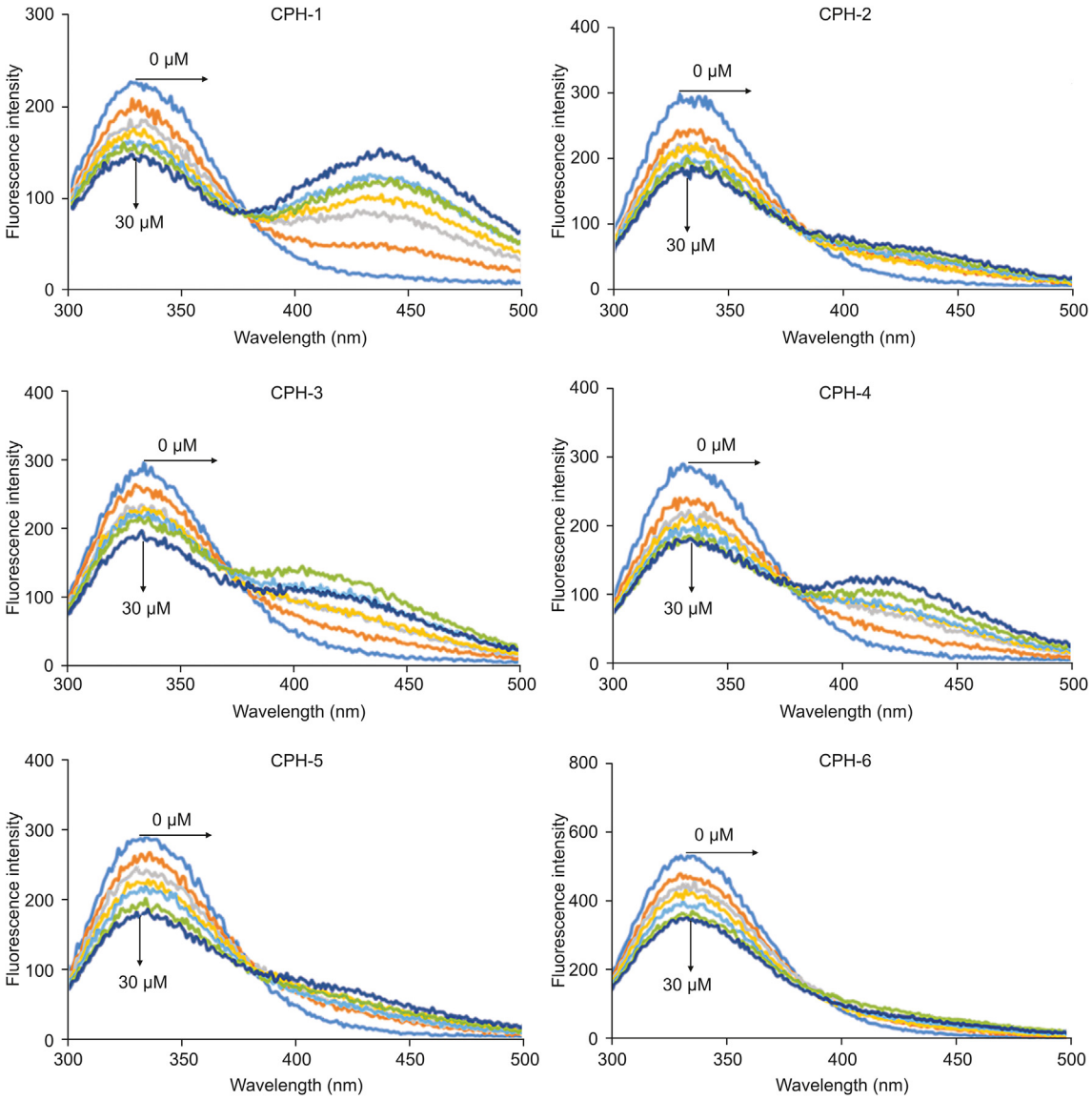

Fig. 3. The changes in the intrinsic fluorescence intensity of $OleT_{SA}$ measured at the excitation wavelength (λ_{em}) of 280 nm in the presence of different concentrations of CPHs (0, 5, 10, 15, 20, 25, and 30 μM) at 298 K.

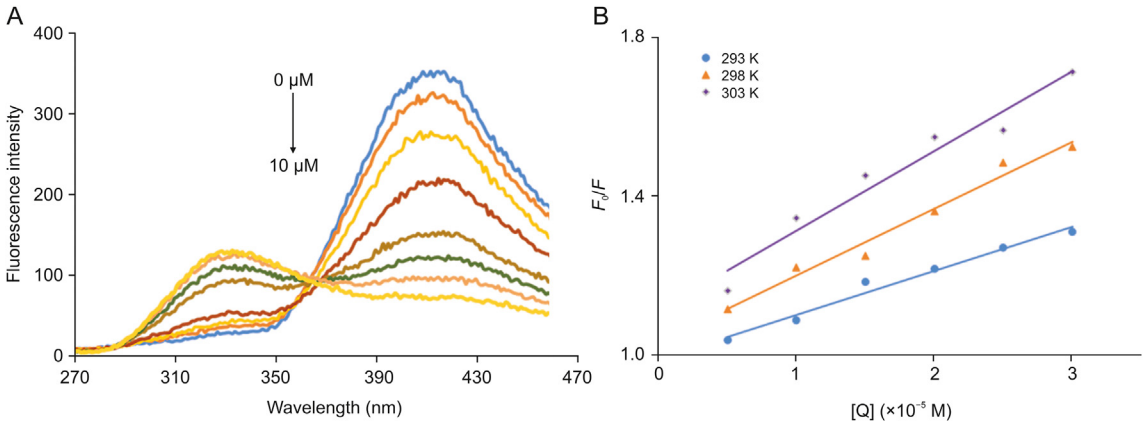

Fig. 4. (A): Fluorescence spectra of CPH-6 measured at the excitation wavelength (λ_{em}) of 250 nm alongside with various concentrations of $OleT_{SA}$ (0, 0.2, 0.6, 2, 4, 6, 8, and 10 μM) at 298 K. (B): Stern-Volmer plot for binding $OleT_{SA}$ with CPH-6 at 293, 298, and 303 K, respectively.

Table 1
Stern-Volmer quenching constants of $OleT_{SA}$ and CPH-6 at 293 K, 298 K, and 303 K.

System	Temp. (K)	K_{sv} (M^{-1}) × 10^{-2}	K_q ($M^{-1}s^{-1}$) × 10^6	R [a]
$OleT_{SA}$-CPH-6	293	11.1	11.1	0.9786
$OleT_{SA}$-CPH-6	298	16.9	16.9	0.9777
$OleT_{SA}$-CPH-6	303	20.1	20.1	0.9523

[a] Correlation coefficient.

Table 2
Binding constants and the number of binding sites on $OleT_{SA}$ for CPH-6.

System	Temp. (K)	K (M^{-1}) × 10^4	n	R [a]
$OleT_{SA}$-CPH-6	293	15.2	1.25	0.9805
$OleT_{SA}$-CPH-6	298	0.40	0.86	0.9788
$OleT_{SA}$-CPH-6	303	0.28	0.79	0.9693

[a] Correlation coefficient.

Volmer constant values was observed with increasing temperatures, indicating that the dynamic quenching was responsible for the quenching process of $OleT_{SA}$ and CPH-6.

The binding constant *(K)* for OleT interaction with CPH-6 and the number of binding sites were described by double logarithmic plots as follows (Eq. (3)) [45,46].

$$\log\frac{F_0 - F}{F} = \log K + n\log[OleT] \quad (3)$$

Here, F_0 and F represent the fluorescence intensities of OleT without and with a quencher, K denotes the binding constant of $OleT_{SA}$ with CPH-6, and n represents the number of binding sites. The characteristic binding parameters K and n were obtained from the plots of log ((F_0–F)/F) versus log [$OleT$] (Fig. 5).

As shown in Table 2, the value of n at the tested temperatures was around equal to one, which demonstrated that there was a single set equivalent binding site in $OleT_{SA}$ with CPH-6. In addition, the value of K is estimated to be 15.2 × 10^4 M^{-1} at 293 K, suggesting a moderately binding affinity between these two substances. A decrease was obtained in the value of K with the increase of temperature from 293 K to 303 K, indicating that the protein can better accommodate the molecule at 293 K than the other two temperatures and the stability between them decreases with increased temperature.

3.2. Thermodynamic analysis

It is well studied that non-covalent interactive forces including hydrogen bonding, hydrophobic interactions, van der Waals force and electrostatic attraction contribute to the binding of small molecules with biomacromolecules [47–49]. Ross and Subramanian [47] reported the main binding forces based on the sign and magnitude of thermodynamic parameters such as enthalpy change (ΔH) and entropy change (ΔS). The principle includes: a) ΔH > 0 and ΔS > 0, hydrophobic forces; b) ΔH < 0 and ΔS < 0, van der Waals interactions and hydrogen bonds; c) ΔH < 0 and ΔS > 0, electrostatic interactions. The ΔH and ΔS are calculated from the liner Van't Hoff plot (Eq. (4)).

$$lnK = -\frac{\Delta H}{RT} + \frac{\Delta S}{R} \quad (4)$$

Here, K shows the associative binding constant at the specific temperature and R is the gas constant. The tested temperatures are 293, 298, and 303 K. ΔH and ΔS are obtained from the slope and intercept of the plot of lnK versus 1/T (Fig. 6). Free energy change (ΔG) is estimated from the following relationship (Eq. (5)).

$$\Delta G = \Delta H - T\Delta S = -RTlnK \quad (5)$$

As shown in Table 3, all the thermodynamic parameters ΔG, ΔH and ΔS were negative at the tested temperatures. Negative values of free energy (ΔG) revealed that the binding of $OleT_{SA}$ with CPH-6 was spontaneous. Both the values of ΔH and ΔS were negative, indicating that the main forces in the $OleT_{SA}$-CPH-6 complex binding were hydrogen bond and van der Waals force.

3.3. UV–vis spectrum analysis

It has been well established that UV–vis spectra of P450s are sensitive to the redox state of the heme as well as its local environment [50]. To further study the binding effect of CPH-6 to $OleT_{SA}$, the spectrum of $OleT_{SA}$ was monitored by UV–vis with or without of CPH-6. As shown in Fig. 7, the fluorescence intensity of $OleT_{SA}$ with 25 μM or 50 μM CPH-6 was adjusted by the extraction of the background fluorescence of corresponding concentration of substrate to eliminate the interference. It was found that the substrate-free $OleT_{SA}$ was in the mixed state at the beginning and the addition of 25 μM CPH-6 led to a slight increase of high spin. With a higher concentration (50 μM), this increment went further, indicating that CPH-6 can alter the microenvironment of heme iron of $OleT_{SA}$.

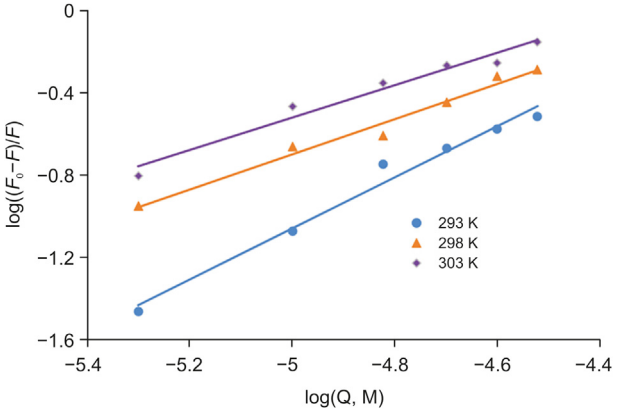

Fig. 5. Double logarithmic plots for $OleT_{SA}$-CPH-6 complexes.

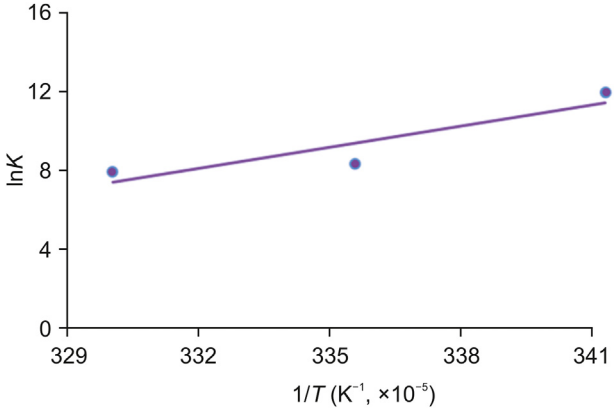

Fig. 6. The Van't Hoff plot for the binding of $OleT_{SA}$ with CPH-6.

Table 3
Thermodynamic parameters for the interaction of $OleT_{SA}$ with CPH-6 at tested temperature.

System	Temp. (K)	ΔH (kJ/mol)	ΔS (kJ/mol·K)	ΔG (kJ/mol)
$OleT_{SA}$-CPH-6	293	−296.1	−915.7	−29.1
$OleT_{SA}$-CPH-6	298	−296.1	−915.7	−20.6
$OleT_{SA}$-CPH-6	303	−296.1	−915.7	−20.0

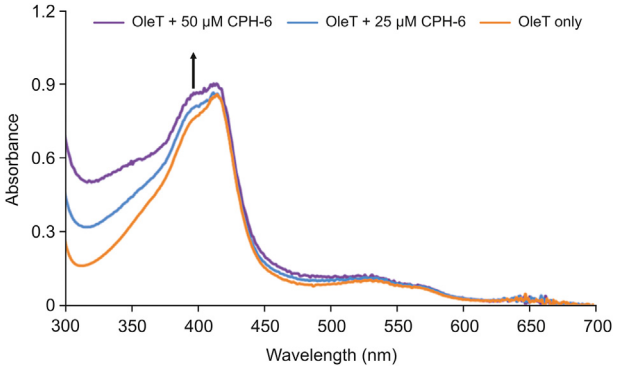

Fig. 7. UV–Vis binding titrations of CPH-6 with $OleT_{SA}$. 10 μM $OleT_{SA}$ was used.

3.4. ^{31}P NMR study

The interactions described above between CPH-6 and $OleT_{SA}$ were confirmed by ^{31}P NMR analysis. As shown in Fig. 8, for the $OleT_{SA}$-CPH-6 complex with 1:1 M ratio, ^{31}P chemical shift value was moved to high field compared to the pure molecule CPH-6, suggesting that the environment of CPH-6 changed after adding into $OleT_{SA}$. As a control, the ^{31}P chemical shift of CPH-6 did not change after incubation with BSA in the same condition. With increased $OleT_{SA}$ concentration (i.e., $OleT_{SA}$-CPH-6 complex with 2:1 M ratio), further shift was observed (Fig. S2). These results confirmed the interaction between $OleT_{SA}$ and CPH-6.

3.5. $OleT_{SA}$ enzymatic activity assay

$OleT_{SA}$ catalyzes the decarboxylation of hydrocinnamic acid to form styrene [51], which can be easily detected by LC. The effect of

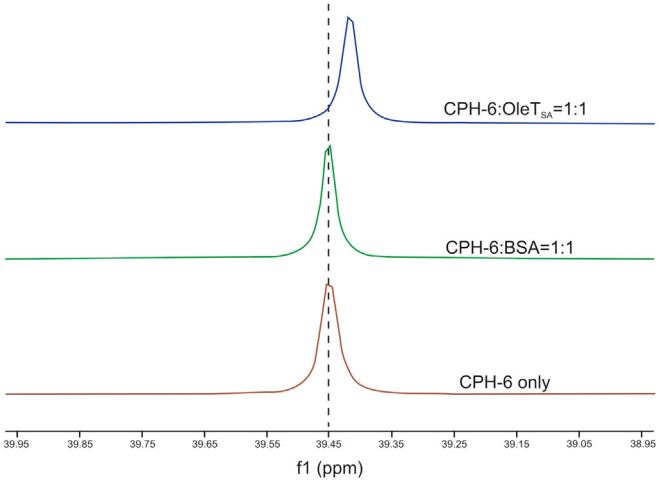

Fig. 8. ^{31}P NMR spectra of CPH-6-$OleT_{SA}$, CPH-6-BSA, and CPH-6 only. 50 μM of $OleT_{SA}$ or BSA, and 50 μM of CPH-6 were used.

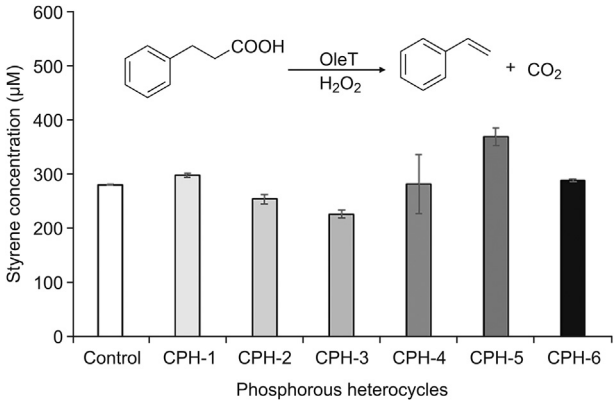

Fig. 9. Different CPHs showed different effects on $OleT_{SA}$ activity (expressed as amount of styrene produced). Reaction condition: 5 μM $OleT_{SA}$, 2 mM hydrocinamic acid, 2 mM H_2O_2, 200 μM CPHs, room temperature for 30 min. Error bars represent standard deviations of duplicate experiments (n=2).

phosphorous heterocycles on $OleT_{SA}$ activity was characterized by using hydrocinnamic acid as substrate (Fig. 9). Interestingly, the CPHs with different side groups showed different effects on $OleT_{SA}$ activity. For example, $OleT_{SA}$ showed around 30% enhanced activity with treatment by CPH-5 (cyclohexyl phosphorous heterocycle with fluoro group) while around 20% activity was inhibited by CPH-3 (cyclopentyl phosphorous heterocycle). Further characterization of enzyme-CPHs complex structure will provide useful information to understand these effects. Nevertheless, the different effects resulting from the fine-tuned small molecule structure represent a viable way to leverage enzyme activity. Such information can be also used for P450 enzyme effector design.

4. Conclusions

In conclusion, this research was to study the interactions between CPHs and $OleT_{SA}$ by fluorescence spectra, UV–vis and ^{31}P NMR spectroscopies. Dynamic quenching mechanism was identified. The binding constant value of 15.2×10^4 M^{-1} at 293 K indicated a moderately binding affinity between CPHs and $OleT_{SA}$. Hydrogen bonding and van der Waals force were identified as main forces involved in the interactions on the basis of thermodynamic parameters analysis. UV–vis spectroscopies suggested that the presence of CPHs could affect the enzyme's interior environment. The ^{31}P NMR studies revealed that binding of CPHs to $OleT_{SA}$ had an influence on the chemical shift of ^{31}P NMR of the molecule. Moreover, the effect of such molecules on $OleT_{SA}$ enzymatic activity indicated potential functions of these molecules and provided useful information for enzyme stimulator design.

Declaration of competing interest

The authors declare that there have no conflicts of interest.

Acknowledgments

This work was supported by the China Scholarship Council and Fujian University-Industry Research Cooperation Project (Project No.: 2018N5013). The authors also wish to thank Thomas M. Makris for providing the OleT plasmid, thank Olivia Manley and Suman Das for their help with protein purification and thank Fiaz Ahmed for offering the help with fluorescence temperature-controlled experiment from Department of Chemistry and Biochemistry of University of South Carolina.

Appendix A. Supplementary data

Supplementary data to this article can be found online at https://doi.org/10.1016/j.jpha.2020.12.004.

References

[1] F.H. Westheimer, Why nature chose phosphates, Science 235 (1987) 1173–1178.
[2] H. Seto, T. Kuzuyama, Bioactive natural products with carbon-phosphorus bonds and their biosynthesis, Nat. Prod. Rep. 16 (1999) 589–596.
[3] G. Zon, Cyclophosphamide analogues, Prog. Med. Chem. 19 (1982) 205–246.
[4] W.J. Stec, Cyclophosphamide and its congeners, Organophosphorus Chemistry, Cambridge: Royal Society of Chemistry, 1982, pp. 145–174.
[5] P. Kafarski, B. Lejczak, Biological activity of aminophosphonic acids, Phosphorus Sulfur Silicon Relat. Elem. 63 (1991) 193–215.
[6] O.M. Colvin, An overview of cyclophosphamide development and clinical applications, Curr. Pharm. Des. 5 (1999) 555–560.
[7] P. Kafarski, B. Lejczak, Aminophosphonic acids of potential medical importance, Curr. Med. Chem. Anticancer Agents 1 (2001) 301–312.
[8] S. Demkowicz, J. Rachon, M. Daśko, et al., Selected organophosphorus compounds with biological activity. Applications in medicine, RSC Adv. 6 (2016) 7101–7112.
[9] J.B. Rodriguez, C. Gallo-Rodriguez, The role of the phosphorus atom in drug design, ChemMedChem 14 (2019) 190–216.
[10] R.J. Richardson, Assessment of the neurotoxic potential of chlorpyrifos relative to other organophosphorus compounds: a critical review of the literature, J. Toxicol. Environ. Health 44 (1995) 135–165.
[11] C.N. Pope, S. Brimijoin, Cholinesterases and the fine line between poison and remedy, Biochem. Pharmacol. 153 (2018) 205–216.
[12] V. Gilard, R. Martino, M. Malet-Martino, et al., Chemical stability and fate of the cytostatic drug ifosfamide and its N-dechloroethylated metabolites in acidic aqueous solutions, J. Med. Chem. 42 (1999) 2542–2560.
[13] E. Budzisz, E. Brzezinska, U. Krajewska, et al., Cytotoxic effects, alkylating properties and molecular modelling of coumarin derivatives and their phosphonic analogues, Eur. J. Med. Chem. 38 (2003) 597–603.
[14] M.D. Sørensen, L.K.A. Blæhr, M.K. Christensen, et al., Cyclic phosphinamides and phosphonamides, novel series of potent matrix metalloproteinase inhibitors with antitumour activity, Bioorg. Med. Chem. 11 (2003) 5461–5484.
[15] S.L. Patil, C.M. Bhalgat, S. Burli, et al., Synthesis, antibacterial and antioxidant properties of newer 3-(1-benzofuran-2-yl)-5-substituted aryl-1, 2-oxazole, Int. J. Chem. Sci. Appl. 1 (2010) 42–49.
[16] L. Clarion, C. Jacquard, O. Sainte-Catherine, et al., Oxaphosphinanes: new therapeutic perspectives for glioblastoma, J. Med. Chem. 55 (2012) 2196–2211.
[17] S. Roy, R.K. Nandi, S. Ganai, et al., Binding interaction of phosphorus heterocycles with bovine serum albumin: a biochemical study, J. Pharm. Anal. 7 (2017) 19–26.
[18] S. Roy, S.K. Saxena, S. Mishra, et al., Spectroscopic evidence of phosphorous heterocycle–DNA interaction and its verification by docking approach, J. Fluoresc. 28 (2018) 373–380.
[19] I.G. Denisov, T.M. Makris, S.G. Sligar, et al., Structure and chemistry of cytochrome P450, Chem. Rev. 105 (2005) 2253–2277.
[20] F.P. Guengerich, Characterization of human cytochrome P450 enzyme, Faseb. J. 6 (1992) 745–748.
[21] P. Anzenbacher, E. Anzenbacherová, Cytochromes P450 and metabolism of xenobiotics, Cell, Mol. Life Sci. 58 (2001) 737–747.
[22] D.C. Lamb, M.R. Waterman, S.L. Kelly, et al., Cytochromes P450 and drug discovery, Curr. Opin. Biotechnol. 18 (2007) 504–512.
[23] A. Veith, B. Moorthy, Role of cytochrome P450s in the generation and metabolism of reactive oxygen species, Cytochromes P450 and drug discovery, Curr. Opin. Toxicol. 7 (2018) 44–51.
[24] M. Foroozesh, J. Sridhar, N. Goyal, et al., Coumarins and P450s, studies reported to-date, Molecules 24 (2019), 1620.
[25] E. Stjernschantz, N.P.E. Vermeulen, C. Oostenbrink, Computational prediction of drug binding and rationalisation of selectivity towards cytochromes P450, Expert. Opin. Drug Metab. Toxicol. 4 (2008) 513–527.
[26] C.C. Ogu, J.L. Maxa, Drug interactions due to cytochrome P450, Proc (Bayl Univ Med Cent) 13 (2000) 421–423.
[27] S. Prasad, S. Mazumdar, S. Mitra, Binding of camphor to *Pseudomonas putida* cytochrome $P450_{cam}$: steady-state and picosecond time-resolved fluorescence studies, FEBS Lett. 477 (2000) 157–160.
[28] V.V. Shumyantseva, T.V. Bulko, N.A. Petushkova, et al., Fluorescent assay for riboflavin binding to cytochrome P450 2B4, J. Inorg. Biochem. 98 (2004) 365–370.
[29] J. Shao, J. Chen, T. Li, et al., Spectroscopic and molecular docking studies of the in vitro interaction between puerarin and cytochrome P450, Molecules 19 (2014) 4760–4769.
[30] G.A. Marsch, B.T. Carlson, F.P. Guengerich, 7,8-benzoflavone binding to human cytochrome P450 3A4 reveals complex fluorescence quenching, suggesting binding at multiple protein sites, J. Biomal. Struct. Dyn. 36 (2018) 841–860.
[31] D. Ma, J. Pan, L. Yin, et al., Copper-catalyzed direct oxidative C–H functionalization of unactivated cycloalkanes into cycloalkyl benzo[*b*]phosphole oxides, Org. Lett. 20 (2018) 3455–3459.
[32] M.A. Rude, T.S. Baron, S. Brubaker, et al., Terminal olefin (1-Alkene) biosynthesis by a novel P450 fatty acid decarboxylase from *Jeotgalicoccus* species, Appl. Environ. Microbiol. 77 (2011) 1718–1727.
[33] C.H. Hsieh, X. Huang, J.A. Amaya, et al., The enigmatic P450 decarboxylase OleT is Capable of, but evolved to frustrate, oxygen rebound chemistry, Biochemistry 56 (2017) 3347–3357.
[34] C. Lu, F. Shen, S. Wang, et al., An engineered self-sufficient biocatalyst enables scalable production of linear alpha olefins from carboxylic acids, ACS Catal. 8 (2018) 5794–5798.
[35] C.E. Wise, C.H. Hsieh, N.L. Poplin, et al., Dioxygen activation by the biofuel-generating cytochrome P450 OleT, ACS Catal. 8 (2018) 9342–9352.
[36] J.A. Amaya, C.D. Rutland, T.M. Makris, Mixed regiospecificity compromises alkene synthesis by a cytochrome P450 peroxygenase from *Methylobacterium populi*, J. Inorg. Biochem. 158 (2016) 11–16.
[37] J.A. Amaya, Mechanisms of Decarboxylation in the CYP152 Family of Cytochrome P450s (Dissertation), University of South Carolina, Los Angeles, USA, 2018.
[38] Y. Chen, M.D. Barkley, Toward understanding tryptophan fluorescence in proteins, Biochemistry 37 (1998) 9976–9982.
[39] A. Sharma, S.G. Schulman, Introduction to Fluorescence Spectroscopy, Wiley Press, New York, 1999.
[40] C. Pontremoli, N. Barbero, G. Viscardi, et al., Insight into the interaction of inhaled corticosteroids with human serum albumin: a spectroscopic-based study, J. Pharm. Anal. 8 (2018) 37–44.
[41] P. Sindrewicz, X. Li, E.A. Yates, et al., Intrinsic tryptophan fluorescence spectroscopy reliably determines galectin-ligand interactions, Sci. Rep. 9 (2019), 11851.
[42] J.R. Lakowicz, Principle of Fluorescence Spectroscopy, Springer, New York, 1999.
[43] J.R. Lakowic, G. Weber, Quenching of fluorescence by oxygen. A probe for structural fluctuations in macromolecules, Biochemistry 12 (1973) 4161–4170.
[44] A.T. Buddanavar, S.T. Nandibewoor, Multi-spectroscopic characterization of bovine serum albumin upon interaction with atomoxetine, J. Pharm. Anal. 7 (2017) 148–155.
[45] V. Anbazhagan, R. Renganathan, Study on the binding of 2,3-diazabicyclo [2.2.2]oct-2-ene with bovine serum albumin by fluorescence spectroscopy, J. Lumin. 128 (2008) 1454–1458.
[46] J. Min, X. Meng-Xia, Z. Dong, et al., Spectroscopic studies on the interaction of cinnamic acid and its hydroxyl derivatives with human serum albumin, J. Mol. Struct. 692 (2004) 71–80.
[47] P.D. Ross, S. Subramanian, Thermodynamics of protein association reactions: forces contributing to stability, Biochemistry 20 (1981) 3096–3102.
[48] G. Némethy, H.A. Scheraga, Structure of water and hydrophobic bonding in proteins. I. A model for the thermodynamic properties of liquid water, J. Chem. Phys. 36 (1962) 3382–3400.
[49] N. Shahabadi, A. Fatahi, Multispectroscopic DNA-binding studies of a tris-chelate nickel(II) complex containing 4,7-diphenyl 1,10-phenanthroline ligands, J. Mol. Struct. 970 (2010) 90–95.
[50] A. Luthra, I.G. Denisov, S.G. Sligar, Spectroscopic features of cytochrome P450 reaction intermediates, Arch. Biochem. Biophys. 507 (2011) 26–35.
[51] A.W. Munro, K.J. McLean, J.L. Grant, et al., Structure and function of the cytochrome P450 peroxygenase enzymes, Biochem. Soc. Trans. 46 (2018) 183–196.